

MECHANICAL BEHAVIOUR AND PRACTICAL ADHESION AT A BAMBOO COMPOSITE INTERFACE: PHYSICAL ADHESION AND MECHANICAL INTERLOCKING

C. A. Fuentes^{a*}, G. Brughmans^b, L.Q.N Tran^c, C. Dupont-Gillain^d, I. Verpoest^a, A.W. Van Vuure^a

^a*Department of Materials Engineering, KU Leuven, Leuven, Belgium*

^b*Campus GroupT, KU Leuven, Leuven, Belgium*

^c*Singapore Institute of Manufacturing Technology, Agency for Science, Technology and Research, Singapore*

^d*Institute of Condensed Matter and Nanosciences, Université Catholique de Louvain, Louvain-la-Neuve, Belgium*

**Carlos.Fuentes@mtm.kuleuven.be*

Abstract

Physical adhesion was experimentally determined by measuring contact angles with different liquids on bamboo and glass fibers, using the Wilhelmy technique, and by applying the acid-base theory for calculating the surface energy components and the theoretical work of adhesion. The mechanical strength of the interfaces was assessed by single fibre pull-out tests. In order to consider the real mechanisms of interfacial failure of natural fiber composites, the fibre matrix interfacial bond strength was characterized by the critical local value of interfacial shear stress, τ_d , and the radial normal stress at the interface, σ_{ult} , at the moment of crack initiation. Both interfacial parameters are used for correlating thermodynamic work of adhesion and practical adhesion. Pull-out tests (taking into account friction), XPS, and profilometry techniques were used to study the influence of rough natural fibre surfaces on the interface between the fibre and a thermoplastic matrix, by comparing the mechanical behaviour at the interface of a smooth optical glass fibre with that of rough natural fibres. The results suggest that the physical and chemical compatibility between the bamboo fibre and the matrix does not improve substantially the composite performance if compared with glass composites. The relatively low off-axis strength of the bamboo fibres is suggested as the main reason for the low stress transfer capability at the fibre-matrix interphase. Furthermore, the pull-out process may be friction-dominated in bamboo fibre systems.

Keywords: Natural fibres; B. Interface; B. Fibre-matrix bond; B. Debonding; C. Failure criterion

1. INTRODUCTION

With the increasing demand for natural fibre reinforced composites, a lot of effort is put in improving their mechanical properties. The weakest part of these composites is often the fibre-matrix interface. This weakness is usually attributed to a bad compatibility between the typically hydrophilic reinforcing fibre and in particular hydrophobic thermoplastic matrices. To achieve a composite with good mechanical properties, a strong fibre-matrix adhesion has to be obtained by interfacial interactions, including mechanical interlocking, chemical bonding and physical adhesion.

A quantitative estimation of physical adhesion is possible by wetting analysis, while mechanical and chemical interactions can only indirectly be estimated from destructive micromechanical tests (micro-indentation, pull-out, etc.). However, micromechanical experiments measure “practical adhesion”, which not only represents purely physical and chemical interactions at the interface. Certainly, the load transfer between the fibre and the matrix also depends on the mechanical properties of both, the fibre and the matrix, and can also be affected by local stresses, matrix residual stresses (processing conditions), presence of easy fracture sites, and the mode of applying external stresses [1, 2]. Hence, micromechanical tests not only measure surface interactions but interdependent interface characteristics. Moreover, typical tests characterise the interfacial shear stress which is parallel to the fibre surface, while the adhesion strength is defined as the work required to separate the matrix from the fibre under loading perpendicular to fibre surface [1].

The pull out test is a widely used technique to characterize the mechanical behaviour of the interface between a matrix and a reinforcing fibre in a composite. Theoretical analyses have been developed to study the fibre pull-out process, and these can be divided into two different approaches, using different failure criteria: energy-based and stress-based criteria. The first approach considers that debonding is the result of crack propagation along the interface, presenting the energy release rate (G_i) for

interfacial crack growth as the failure criterion. The second approach is based on failure at interfacial shear stress. This approach has evolved, using the local shear stress (derived from the “kink” force, where debonding starts) instead of the average stress (derived from the peak force), and considers the local adhesional shear strength value (τ_d) as the intrinsic interface property that characterizes the strength of the fibre-matrix interface [3, 4]. Both approaches have been proved to be practically equivalent, and they both can predict the debond force as a function of the embedded fibre length [5].

As it was mentioned before, τ_d or G_{ic} are measured under shear loading, parallel (mode II) to the fibre surface while the work of adhesion (W_a) is defined under perpendicular loading conditions (mode I). Since it has been demonstrated that during crack initiation in the pull-out test the crack surfaces move directly apart [6, 7], Pisanova et al. [1] suggest the possibility to correctly relate W_a with the normal stress at the debond point. The latter can be calculated using the analytical expressions derived by Nairn and Sheer for the analysis of all stresses in a pull-out specimen [8, 9], and the results obtained from pull-out tests.

The aim of this paper is to study the influence of physical adhesion and roughness on the mechanical behaviour of interfaces between a bamboo natural fibre and a polypropylene (PP) and a polyvinylidene fluoride (PVDF) matrix. For comparing the mechanical behaviour at the interface of a smooth fibre with that of rough natural fibres, optical glass fibres were used since they possess a very smooth surface, and constant cross section along the fibre direction, which makes it ideal for reducing the effect of mechanical interlocking. Physical adhesion was experimentally determined by measuring contact angles with different liquids using the Wilhelmy technique and by applying the acid-base theory for calculating the surface energy components and the wetting parameters.

2. MATERIALS AND METHODS

2.1 Materials

The silica core (diameter: 200 μm) of optical glass fibres from Thorlabs (FR200UMT) were used in this study. Technical bamboo fibres of the species *Guadua angustifolia* were mechanically extracted from bamboo culms in the Department of Materials Engineering at KULeuven. Polypropylene (PP) and polyvinylidene fluoride (PVDF, Solef 1008) were obtained from Propex, and Solvay respectively in the form of films. The selection of these matrices is based on the difference of surface energies between PP (non-polar) and PVDF (polar).

2.2 Materials preparation

Only the silica core of the optical glass fibres is needed, and thus the outer layers have to be removed. The cladding layer is removed by submerging the stripped fibres in hot sulphuric acid. The fibres were submerged in piranha solution (mixture of concentrated sulphuric acid and hydrogen peroxide) for 30 minutes. Finally, the glass fibres were rinsed off with water and stored in ultrapure water (resistivity > 18M Ω .cm) for avoiding environmental organic contamination. A consistent cleaning of the fibre surface guarantees the same surface chemistry for all the samples, avoiding the chemical or physical interaction of unknown elements during the pull-out tests.

Bamboo fibres were cleaned with warm water for one hour (90°C), then wiped with ethanol with a piece of cotton tissue before being dried in a vacuum oven at 80°C for one hour. The fibres were then stored at room conditions (60% RH, 20 °C).

2.3 Contact angle measurements and surface energy analysis

Advancing and receding contact angles of various test liquids (ultrapure water: 18.2 Ω cm resistivity, diiodomethane: Merck, and ethylene glycol: Sigma–Aldrich) were measured on the polymer films and glass fibres under controlled conditions (temperature of 20°C and humidity of 60%), with a Krüss K100 tensiometer using the Wilhelmy technique [10, 11]. In order to better describe both the low surface energy and the high surface energy components of the analysed surfaces, the average of the cosines of the

advancing (θ_{adv}) and receding (θ_{rec}) angles was used for the glass fibres to estimate the cosine of the equilibrium angle (θ_{equ}), as has been suggested by Andrieu et al.[12], and is shown in Equation 1.

$$\cos \theta_{equ} = 0.5 \cos \theta_{adv} + 0.5 \cos \theta_{rec} \quad (1)$$

For the case of bamboo fibres, equilibrium contact angles were measured directly by using acoustic vibration, as it was shown in our previous publication [13].

For evaluating the effect of organic molecules from the air on the surface of glass, some contact angles were measured immediately after the optical fibre were cleaned, and some others after being exposed to our lab environment for a certain period of time.

Surface energy components were calculated according to the Van Oss model and by using the SurfTen 4.3 software developed by Claudio Della Volpe [14]. Also, the work of adhesion (W_a), the spreading coefficient (S), the wetting tension (ΔF), and the interfacial energy (γ_{sl}), which are wetting parameters related to the interfacial strength [15], are calculated according to the following equations:

$$W_a = \gamma_s + \gamma_l - \gamma_{sl} = \gamma_l(1 + \cos \theta) \quad (2)$$

$$S = \gamma_s - (\gamma_l + \gamma_{sl}) \quad (3)$$

$$\Delta F = \gamma_s - \gamma_{sl} = \gamma_l \cos \theta \quad (4)$$

$$\gamma_{sl} = \left(\sqrt{\gamma_s^{LW}} - \sqrt{\gamma_l^{LW}} \right)^2 + 2 \left(\sqrt{\gamma_s^+} - \sqrt{\gamma_l^+} \right) \left(\sqrt{\gamma_s^-} - \sqrt{\gamma_l^-} \right) \quad (5)$$

2.4 Roughness

The roughness of glass and bamboo fibre surface was measured with a WYKO NT3300 profilometer. In combination with a microscope, it allows roughness measurement of surfaces. The spatial sampling interval ranges from approximately 0.1 μm to 10 μm .

2.5 Surface characterization: X-ray photoelectron spectroscopy (XPS)

XPS analyses were performed on a Kratos Axis Ultra spectrometer (Kratos Analytical – Manchester – UK) equipped with a monochromatized aluminium X-ray source (powered at 10 mA and 15 kV). More information regarding the XPS analysis procedure can be found in our previous publication [10].

2.6 Pull-out test

2.6.1 Sample preparation: A block of polymer was put in an aluminium cylindrical container with a radius of 5 mm and heated until melting temperature. When the polymer was completely molten, the fibre (glass and bamboo) is placed perpendicular to the polymer surface and in its centre with the help of an optical microscope to guarantee accuracy. The embedded length was controlled in the following way: when the fibre entered in contact with the molten polymer, it was pushed down to a certain depth driven by a micrometer with an accuracy of 5 μm . After the fibre was placed, the specimen was cooled down at a rate of 4°C/min until it reached room temperature. The processing temperatures used were 200°C for PP and 220°C for PVDF.

To perform the pull-out test, the aluminium holder containing the polymer and the fibre is attached to the load cell of an Instron 5943 mini tensile machine. It is important to carefully position the block of polymer since the area where the blades touch the upper surface of the block plays an important role concerning the induced compressive stress profile in the specimen. A fibre free length of 5 mm was chosen for all the specimens.

2.6.2 Evaluation of the interfacial strength: The typical apparent interfacial shear strength IFSS (τ_{app}) is only an average stress, which depends on the embedded length and does not take into account neither the influence of interfacial friction in already debonded regions nor the shear stress variations in the bonded regions. In order to consider the real mechanisms of interfacial failure, Zhandarov and several other researchers [3, 5, 16] proposed to characterize the fibre matrix interfacial bond strength by the critical local value of interfacial shear stress, τ_d . This is defined as the stress at which local debonding of the fibre from

the matrix takes place. At this stage the recorded force will continue increasing since the crack growth is stabilised by the friction between fibre and matrix in the debonded area (interfacial friction, τ_f), until the crack becomes unstable at a finite crack length, a .

In the force-displacement curve (Fig.1-left), the visible ‘kink’ corresponds to the start of debonding at the interface or crack initiation. This crack propagates along the interface while the pull-out force increases and the fibre slides out from the matrix, with friction acting between the recently debonded surfaces. Accordingly, the peak force, F_{max} , can be much higher than the kink or debond force, F_d , depending on the relationship between adhesion and friction in the specific fibre-matrix system. Thus, the debond force is a key parameter to characterize the strength of a fibre-matrix system. However, generally this debond force is difficult to determine by usual techniques like the recording of the force-displacement curve or by monitoring the crack propagation; then the only reliable measured load value is F_{max} .

2.6.3 Estimation of τ_d and τ_f by fitting theoretical $F_{max}(l_e)$ to experimental data

Zhandarov et al. [17] developed an algorithm which makes possible to determine the critical IFSS, τ_d , and to estimate interfacial friction, τ_f , from the maximum load value recorded in the pull-out test. This is possible by performing measurements over a wide range of embedded lengths, l_e . To reduce the influence of friction, short embedded lengths should be obtained depending on the diameter of the fibre.

Based on the shear lag model of stress transfer to the matrix, and assuming that for any current crack length, a , the shear stress at the crack tip, $\tau_{(a)}$, is constant ($\tau_{(a)} = \tau_d = const$); Zhandarov et al. [5] have developed a model to describe the current applied force, F , as a function of the crack length, a .

$$F = \frac{\pi d}{\beta} \left\{ \tau_d \tanh[\beta(l_e - a)] - \tau_T \tanh[\beta(l_e - a)] \tanh \left[\frac{\beta(l_e - a)}{2} \right] + \beta a \tau_f \right\} \quad (6)$$

Where τ_T is the residual stress due to thermal shrinkage, τ_f is the frictional stress in the already debonded region, and β is the corrected shear-lag parameter according to Nairn [18].

Due to the difference between the coefficients of thermal expansion of the fibre and the matrix, the latter accumulates residual stress during cooling from processing temperatures, affecting the interfacial strength.

$$\tau_T = \frac{\beta r_f E_f}{2} (\alpha_f - \alpha_m) \Delta T \quad (7)$$

Where E_f is the longitudinal tensile modulus of the fibre (46.6 GPa for the optical glass fibres, which was measured by an optical extensometer, and 40.0 GPa for bamboo fibres according to [19]), r_f is the radius of the fibre, α_f and α_m are the longitudinal coefficients of thermal expansion (CTE) of the fibre and the matrix respectively (5, 60, 70, and $120 \times 10^{-6}/K$ for glass, bamboo, PP, and PVDF respectively, considering the properties of lignin for bamboo fibres since it is covered by a lignin layer [10]), and ΔT is the difference between the test temperature and the stress-free temperature (116 and 142 °C for PP and PVDF respectively).

The total debonding of the fibre from the matrix occurs at the recorded peak force F_{max} (see Figure 1). The force up to that moment reflects a combined resistance from friction in already debonded areas and adhesion in the still adhered section. The value of F_{max} can be used to obtain τ_d and τ_f by fitting experimental data according to the algorithm developed by Zhandarov et al. [17], and by using our own built code in Python language.

2.6.4 Estimation of adhesional pressure σ_{ult}

The adhesional stress calculation is based on the analysis of the stresses (axial, radial and shear) in a microdroplet debond specimen by Scheer and Naim [9] using a variational mechanics analysis. The results of the stress state calculation suggest that the interfacial failure between the fibre and the matrix may be by mode I at the beginning of the sample. This failure is caused by a large tensile radial stress at the fibre-matrix interface, with a zero shear stress, where the fibre enters the matrix while the radial stress,

is maximum (see Fig.1-right). The latter is in agreement with experimental and finite element analysis reported in literature [1, 6, 7].

The radial tensile stress, σ_{ult} , balances the interfacial pressure produced by adhesive forces at the exact moment when debonding takes place, and therefore is directly proportional to the theoretical work of adhesion (W_a). According to Pisanova et al. [20], W_a can be expressed as follows:

$$W_a = \sigma_{ult} \lambda \quad (8)$$

where λ is the effective normal displacement between the contacting surfaces required for their separation. The latter can also be considered as the effective range of action of intermolecular forces, which depends on the chemical nature of a given fibre-matrix system [21].

The detailed equations for the calculation of the adhesional pressure are given by Sheer and Nairn [9] and adapted by Pisanova [20]. The calculation of this critical normal interface stress at the moment of interface failure (σ_{ult}) includes the fibre axial stress at the debond point at the moment of crack initiation, ψ_p , and its second derivative with respect to the axial coordinate. The solution consists of several mathematical operations which are described in [9] [20]. The calculations were done again by executing a self-written Python program and the DerApproximator package for getting derivatives via finite-difference approximation. For this analysis a cylindrical microdroplet specimen with volume fraction $V_f = 0.05$ and $l_e = 1$ mm (at higher values of l_e , the variation of σ_{ult} is less than 2 %) were assumed.

Accordingly, the influence of physical adhesion and roughness on the interface strength will be characterized by two different approaches: the local interface shear strength (τ_d and τ_f), and the normal interface stress at the moment of crack initiation (σ_{ult}). These results will be contrasted with the work of adhesion obtained by wetting measurements.

3 RESULTS AND DISCUSSION

3.1 Roughness and wetting behaviour of glass fibres

The roughness of the cleaned glass fibre was measured using a profilometer, and contact angle measurements of water on glass fibres are used to prove the quality of the cleaned surface, verified by XPS analysis as can be seen further on Table 1. The measured roughness of the cleaned fibre is very low $R_a = 42$ nm, allowing a minor effect of the mechanical interlocking mechanism when studying the interface by pull-out testing. In contrast, the roughness of the bamboo fibres is higher as expected $R_a = 3,2$ μm (two orders of magnitude higher than the cleaned glass fibre), as can be seen in Fig.2.

Regarding the wetting behaviour of glass fibres, both receding and advancing contact angles of water on cleaned fibres vary over time, as can be seen in Fig.3. When contact angles were measured immediately after cleaning, the values were remarkably lower if compared with those after two or three hours (Fig.3). Hence, receding and advancing contact angles of 15 and 36 degrees respectively were measured right after the cleaning procedure, but when the same fibre was exposed to a normal environment and the angles measured one day later, stable receding and advancing contact angles of 50 and 80 degrees were obtained.

This phenomenon is related to the interaction of OH groups on the surface of the fibre with organic molecules from the air and the high surface energy of glass. After the cleaning procedure with sulphuric acid and piranha solution, a group of fibres were stored in ultra-pure water for protecting them against contamination and another group were exposed to normal environmental conditions. The carbon concentration, mainly the C-(C-H) component, is notably higher on samples stored in air than on samples stored into water as it can be seen in the XPS results (see Table 1). Moreover, the C/Si ratio is higher for the samples that were stored in air, which further proves the carbon contamination. Consequently, the glass fibres used for our micro-mechanical tests were stored in ultra-pure water.

3.2 Surface energy components

In Table 2, the surface energy components of the fibres (glass and bamboo) and thermoplastic surfaces (PP and PVDF), calculated from the equilibrium contact angles (using Equation 1), are presented. As expected, PVDF possesses higher acidity due to the different electro-negativities of carbon, fluorine, and hydrogen. In particular, the strong inductive effect of the fluorine atoms polarizes the electronic distribution of partially fluorinated polymers [22]. The results for PET are in accordance with published literature [23] wherein it is classified as a basic polymer due to its ester functional groups. For the case of PP, we find a deviation in the magnitude of the polar surface energy component, which was expected to be zero since pure PP is a nonpolar polymer. This effect could be related to aging processes or surface contamination [24].

The obtained surface energy values for the bamboo fibre (Table 2) may be discussed in the light of the XPS results presented in Table 1. The different contributions of functional groups to the shape of the C1s peak have been described in the literature for lignocellulosic materials [25, 26]: C–(C,H) linkages of lignin and extractives (C1); C–OH groups of cellulose, hemicelluloses, lignin and extractives, as well as C–O–C linkages of lignin and extractives (C2); C=O groups in lignin and extractives, as well as O–C–O linkages in cellulose and hemicelluloses (C3); COOH groups of hemicelluloses, as well as COOC and COOH groups of extractives (C4).

According to the literature [25, 27, 28], these four different components of the carbon peak may be related to the physical interactions of materials within a measured depth of 5 to 10 nm: C1 may be recognized as representative of aliphatic or aromatic carbon participating in Lifshitz-Van Der Waals interactions; while C2, C3, and C4 might represent polar interactions. The high level of C1 component compared to the others is in agreement with the rather dispersive character of bamboo fibres deduced from the surface energy components (see Table 2).

For the case of clean glass fibres, the O/Si and C/Si ratios correspond well with those reported in literature for glass fibres [29]. It can be seen (Table 2) that glass fibres have a higher basic component than bamboo fibres. This result may be explained by the fact that there are more OH-groups on the surface of clean glass fibres (oxygen concentration is almost twice in glass if compared with bamboo, see Table 1).

Table 3 shows the calculated wetting parameters: work of adhesion (W_a), spreading coefficient (S), wetting tension (ΔF), and interfacial energy (γ_{sl}), for bamboo and glass fibres as substrates, following the equations 2, 3, 4, and 5.

For glass and bamboo fibres as substrates, the PVDF system gives the highest values for W_a and ΔF , and the lowest γ_{sl} , representing the best combination of wetting parameters if compared with PP as a matrix. Also the higher acidic surface energy component of PVDF and the very high basic component of glass and bamboo may explain the good match. However, S in PVDF is low, meaning that the molten matrix would have difficulties to spread on the fibre's surface during the impregnation process.

3.3 Pull-out test

By following the procedure described in 2.6.4, the measured and the theoretical maximum force (F_{max}), blue points and red dotted lines respectively, are plotted as function of the embedded length (l_e) in Figure 4 for glass and bamboo systems. The R^2 values for all the systems are close to one, which may confirm a good correlation of the measured forces. The inserts show the residual plots for better analysing mild deviations of data from the model. The determined interfacial parameters and the theoretical work of adhesion (W_a) are shown in Table 3.

There was a good correlation between the interfacial parameters determined from the pull-out test and the theoretical W_a for glass as substrate. As it can be seen in Table 3 and Figure 5, the value of τ_d for the PVDF-glass fibre system is approximately 5 times higher than the values obtained for the PP-glass

system. The latter clearly indicates a higher interfacial adhesion and greater surface energy components compatibility of PVDF on glass fibres if compared with PP system.

If the two glass fibre systems are analysed together, the obtained τ_f value for the PVDF is lower than those for PP (see Table 3). For short embedded lengths (< 2 mm), F_{max} for the PVDF system is higher due to its high τ_d ; but as the embedded length increases also the influence of friction does, reducing the force needed to pull out the fibre (due to lower friction of the debonded region) as it can be seen in Fig.6-left, where the theoretical curves are analysed. If friction is not taken into account, the performance of the PVDF-glass system is always the best (see Figure 6-right).

Even though the roughness of the fibres was the same for the 2 glass systems, the effect of friction is lower in PVDF than in the PP system. As it is shown in Table 3, τ_f is low for the PVDF system. This may be related to the difficulty of PVDF to spread on the glass surface due to its low spreading coefficient (see Table 3), reducing the amount of area in contact with the glass surface and also reducing the mechanical interlocking, as the matrix does not penetrate that well into the surface roughness.

The calculation of the interfacial parameters from pull-out tests for bamboo fibres was more complicated. It is well known that bamboo fibres do not have a circular cross-section, the cross section changes along the fibre length and each fibre possesses a different perimeter [10]. Since the calculation of the pull-out interfacial parameters depends on the assumption of a perfect cylindrical body and the fitting of several maximum forces for different fibres of the same diameter, the results for bamboo are approximations. Bamboo fibres of approximately the same size were carefully selected.

Figure 4 shows F_{max} as a function of the embedded length for a PP and PVDF-bamboo fibre system. The R^2 values for both systems are ~ 0.99 , but the inset for the PVDF system show a relatively considerable deviation of data from the model due to the reasons explained in the previous paragraph (different perimeter and cross-section along the fibre length).

As can be seen in Table 3, τ_d values for bamboo fibre are relatively low if compared with glass fibre systems, while τ_f values are relatively high. The latter indicates that friction plays a major role in bamboo fibre systems: debonding occurs at relatively low forces but friction keeps increasing F_{max} , giving the appearance of good mechanical interfacial properties. F_{max} for bamboo as substrate surpasses the force value obtained for glass as substrate at embedded lengths higher than 1 mm, although τ_d for glass-PP is more than double the value obtained for bamboo-PP, and the value for glass-PVDF is almost 3 times the value for bamboo-PVDF. Contrary to glass systems, the τ_f value obtained for the PVDF-bamboo fibre system is higher than that for bamboo-PP, which may be related to the difference in roughness of two orders of magnitude between bamboo and glass (see section 3.1). In the latter case of bamboo, PVDF may be able to impregnate more surface area due to the relatively big cavities on the fibre surface and the good physical interaction with the fibre, increasing the level of polymer-fibre contact area.

Contrary to expectations, τ_d values are lower for bamboo as substrate than those found for glass, although W_a is higher for bamboo. This result may be explained by the fact that the calculation of the theoretical W_a does not take into account the mechanical properties of the matrix nor the fibre.

These results are consistent with those of Thomason [30] and suggest that natural fibres are not able to deliver the level of stress and load distribution efficiency at the interface that would be expected from their high longitudinal mechanical properties. Furthermore, if PP and MAPP-bamboo composites are compared, the occurring of chemical bonding at the fibre-matrix interface does not appear to provide significant improvement in the performance of natural fibre reinforced PP composites, as it was shown in our previous study [11]. These results may be explained by the anisotropic nature of natural fibres, and particularly bamboo in this study, that provokes a great reduction of their transversal or shear mechanical properties. In this case, the interfacial shear strength is limited by the shear strength of the fibre. As it can be seen in Figure 7, the bamboo fibre fails in the transverse direction, and fragments of its outer layer

surface and even some elementary fibres remains in the pull-out hole; moreover, the pulled-out bamboo fibre surface shows no matrix remaining. In comparison, the pull-out hole left by the glass fibre looks clean, as well as its pulled out fibre surface.

For further analysis, the adhesional pressure (σ_{ult}) was used as criteria for interfacial failure. According to Zhandarov [31], this normal stress component at the matrix interface corresponds to the tensile mechanism of crack initiation, and it is directly proportional to W_a , but considers the mechanical properties of the fibre and the matrix. As it can be seen in Table 3 and Figure 5, σ_{ult} corresponds well with W_a if the analysis is made independently for each fibre.

However, if bamboo and glass systems are compared, again the performance of bamboo is poor. These findings once more support the idea of the anisotropic nature of bamboo fibres (low mechanical properties in the transverse direction which produces the detachment of the outer layer and elementary fibres in contact with the matrix) as the main cause for its low interfacial properties. Even though the chemistry of the surface of the fibre displays good interaction with the matrix, apparently low transversal mechanical properties fail to transfer stress at the interface. This may be related to the limited mechanical properties of lignin which is predominant at the surface of technical bamboo fibres [10].

4 CONCLUSIONS

Practical adhesion in single fibre glass and bamboo composites was evaluated by two different interfacial parameters obtained from pull-out tests: τ_d and σ_{ult} . Both parameters are consistent with the theoretical W_a , if each system (glass and bamboo) is independently analysed. As expected PVDF systems give the best interfacial performance due to high physical interaction between the fibre and the matrix.

When bamboo and glass systems are compared, both interfacial parameters (τ_d and σ_{ult}) show a poor performance for bamboo composites, even though W_a is higher for bamboo. Taken together, these

results suggest that the physical and chemical compatibility between the bamboo fibre and the matrix may not be improving substantially the composite performance if compared with glass composites.

Although the current study is based only on bamboo fibres, the findings suggest the anisotropic nature of natural fibres as the main reason for the low stress transfer capability at the fibre-matrix interphase. Furthermore, the pull-out process may be friction-dominated in bamboo fibre systems.

5 ACKNOWLEDGMENTS

Our thanks to Pierre Eloy and Michel Genet for help with XPS measurements. We would also like to acknowledge the financial support of K.U. Leuven (SBA Scholarship).

6 REFERENCES

- [1] Pisanova E, Zhandarov S, Mäder E. How can adhesion be determined from micromechanical tests? *Composites Part A: Applied Science and Manufacturing*. 2001;32(3):425-434.
- [2] Desaeger M, Verpoest I. On the use of the micro-indentation test technique to measure the interfacial shear strength of fibre-reinforced polymer composites. *Composites Science and Technology*. 1993;48(1):215-226.
- [3] Zhandarov S, Pisanova E, Mäder E, Nairn J. Investigation of load transfer between the fiber and the matrix in pull-out tests with fibers having different diameters. *Journal of Adhesion Science and Technology*. 2001;15(2):205-222.
- [4] Gorbatkina YA, Ivanova-Mumjjeva V. Adhesive strength of fibre/polymer joints upon loading in liquids: effect of liquid surface tension. *International Journal of Adhesion and Adhesives*. 1997;17(4):329-332.
- [5] Zhandarov S, Pisanova E, Lauke B. Is there any contradiction between the stress and energy failure criteria in micromechanical tests? Part I. Crack initiation: stress-controlled or energy-controlled? *Composite Interfaces*. 1997;5(5):387-404.
- [6] Marotzke C. Influence of the fiber length on the stress transfer from glass and carbon fibers into a thermoplastic matrix in the pull-out test. *Composite Interfaces*. 1993;1(2):153-166.
- [7] Piggott M. A new model for interface failure in fibre-reinforced polymers. *Composites Science and Technology*. 1995;55(3):269-276.
- [8] Nairn JA. A variational mechanics analysis of the stresses around breaks in embedded fibers. *Mechanics of Materials*. 1992;13(2):131-154.
- [9] Scheer RJ, Nairn JA. Variational mechanics analysis of stresses and failure in microdrop debond specimens. *Composites Engineering*. 1992;2(8):641-654.
- [10] Fuentes CA, Tran LQN, Dupont-Gillain C, Vanderlinden W, De Feyter S, Van Vuure AW, et al. Wetting behaviour and surface properties of technical bamboo fibres. *Colloids and Surfaces A: Physicochemical and Engineering Aspects*. 2011;380(1-3):89-99.
- [11] Fuentes CA, Tran LQN, Van Hellemont M, Janssens V, Dupont-Gillain C, Van Vuure AW, et al. Effect of physical adhesion on mechanical behaviour of bamboo fibre reinforced

thermoplastic composites. *Colloids and Surfaces A: Physicochemical and Engineering Aspects*. 2012;418:7-15.

[12] Andrieu C, Sykes C, Brochard F. Average spreading parameter on heterogeneous surfaces. *Langmuir*. 1994;10(7):2077-2080.

[13] Fuentes CA, Beckers K, Pfeiffer H, Tran L, Dupont-Gillain C, Verpoest I, et al. Equilibrium contact angle measurements of natural fibers by an acoustic vibration technique. *Colloids and Surfaces A: Physicochemical and Engineering Aspects*. 2014;455:164-173.

[14] Della Volpe C, Brugnara M, Maniglio D, Siboni S, Wangdu T. About the possibility of experimentally measuring an equilibrium contact angle and its theoretical and practical consequences. *Contact angle, wettability and adhesion*. 2006;4:79.

[15] Connor M, Bidaux JE, Manson JAE. A criterion for optimum adhesion applied to fibre reinforced composites. *Journal of materials science*. 1997;32(19):5059-5067.

[16] Pisanova E, Zhandarov S, Mäder E, Ahmad I, Young R. Three techniques of interfacial bond strength estimation from direct observation of crack initiation and propagation in polymer-fibre systems. *Composites Part A: Applied Science and Manufacturing*. 2001;32(3):435-443.

[17] Zhandarov SF, Mäder E, Yurkevich OR. Indirect estimation of fiber/polymer bond strength and interfacial friction from maximum load values recorded in the microbond and pull-out tests. Part I: local bond strength. *Journal of Adhesion Science and Technology*. 2002;16(9):1171-1200.

[18] Nairn J. Generalized shear-lag analysis including imperfect interfaces. *Advanced Composites Letters*. 2004;13(6):263 - 274.

[19] Osorio L, Trujillo E, Van Vuure A, Verpoest I. Morphological aspects and mechanical properties of single bamboo fibers and flexural characterization of bamboo/epoxy composites. *Journal of Reinforced Plastics and Composites*. 2011;30(5):396-408.

[20] Pisanova E, Zhandarov S, Mäder E. How can adhesion be determined from micromechanical tests? *Composites Part A: Applied Science and Manufacturing*. 2001;32(3):425-434.

[21] Zhandarov S, Mäder E. Characterization of fiber/matrix interface strength: applicability of different tests, approaches and parameters. *Composites Science and Technology*. 2005;65(1):149-160.

[22] Lee S, Park JS, Lee TR. The Wettability of Fluoropolymer Surfaces: Influence of Surface Dipoles. *Langmuir*. 2008;24(9):4817-4826.

[23] Gheorghiu M, Pascu M, Popa G, Vasile C, Mazur V. Poly (Ethylene Terephthalate) Films with Different Content of Acid-Base Functionalities. I. Surface Modifications. *International Journal of Polymeric Materials*. 1998;40(3-4):229-256.

[24] Aranberri-Askargorta I, Lampke T, Bismarck A. Wetting behavior of flax fibers as reinforcement for polypropylene. *Journal of colloid and interface science*. 2003;263(2):580-589.

[25] Shen Q, Mikkola P, Rosenholm JB. Quantitative characterization of the subsurface acid-base properties of wood by XPS and Fowkes theory. *Colloids and Surfaces A: Physicochemical and Engineering Aspects*. 1998;145(1-3):235-241.

[26] Johansson LS, Campbell J, Koljonen K, Stenius P. Evaluation of surface lignin on cellulose fibers with XPS. *Applied surface science*. 1999;144:92-95.

[27] Fowkes FM. Quantitative characterization of the acid-base properties of solvents, polymers, and inorganic surfaces. *Journal of adhesion science and technology*. 1990;4(1):669-691.

[28] Lavielle L, Schultz J, Nakajima K. Acid-base surface properties of modified poly (ethylene terephthalate) films and gelatin: Relationship to adhesion. *Journal of applied polymer science*. 1991;42(10):2825-2831.

- [29] Tishchenko GA, Brus J, Dybal J, Pekárek M, Sedláková Z, Bleha M, et al. Surface-Deposited Acid/Base on Glass Microfibers in Formation of (3-Aminopropyl) triethoxysilane-[2-(3, 4-epoxycyclohexyl) ethyl] heptaisobutyl-octasilsesquioxane Biooverlay. *Langmuir*. 2006;22(8):3633-3639.
- [30] Thomason J. Why are natural fibres failing to deliver on composite performance? 17th International Conference on Composite Materials, ICCM17, 2009.
- [31] Zhandarov S, Gorbatkina Y, Mäder E. Adhesional pressure as a criterion for interfacial failure in fibrous microcomposites and its determination using a microbond test. *Composites Science and Technology*. 2006;66(15):2610-2628.

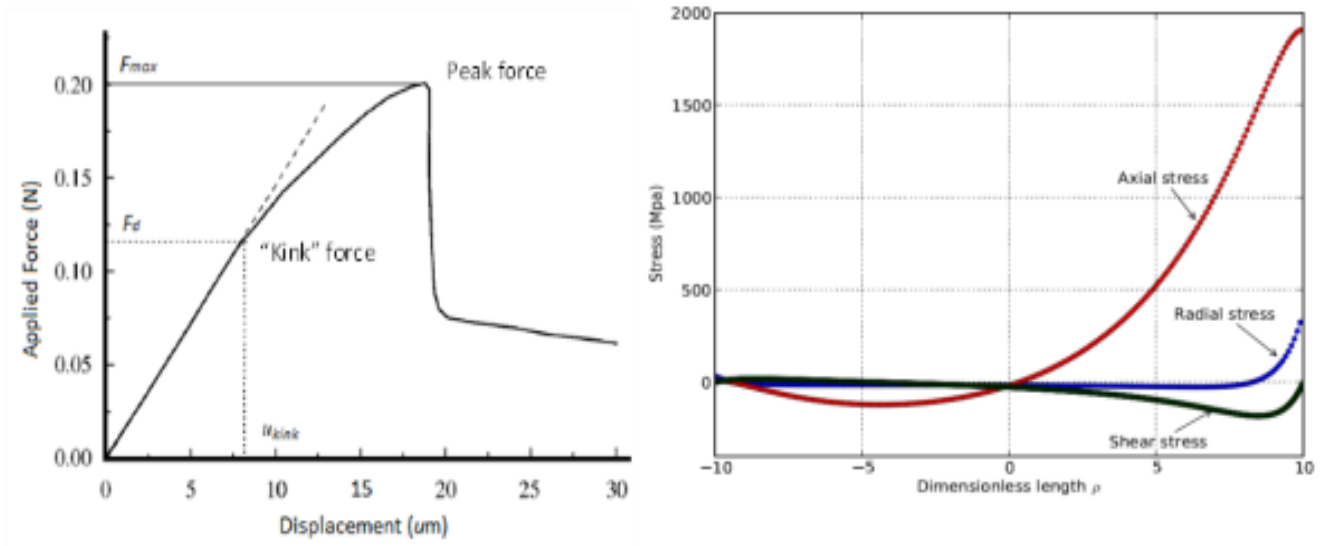


Figure 1. (Left) A pull-out test force-displacement curve [21]. (Right) The fibre axial stress, interfacial shear stress, and interfacial shear stress along the embedded length in a pull-out test. The horizontal axis is the distance from the specimen midpoint of dimensionless length 2ρ to the knife edges [9].

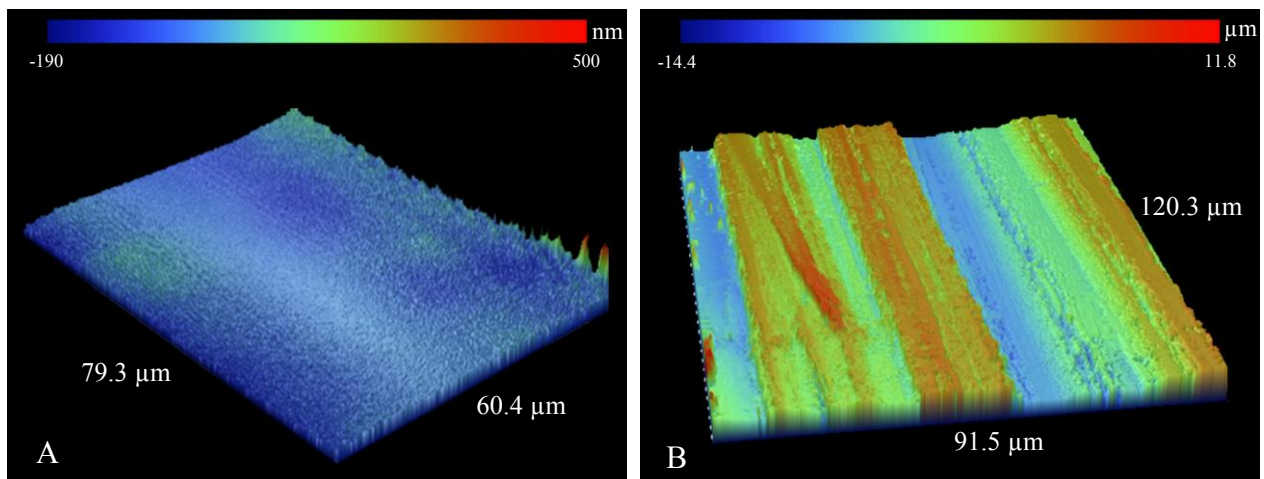


Figure 2. Three dimensional profile of fibre surface by profilometer: (A) glass fibre surface was cleaned with sulphuric acid and piranha solution, and (B) bamboo fibre surface.

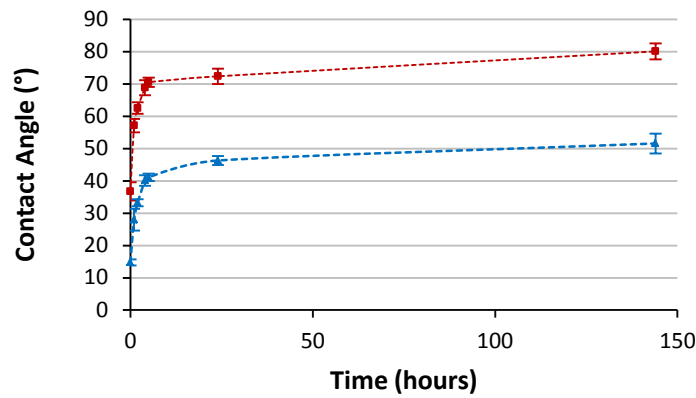


Figure 3. Variation of the advancing (red squares) and receding contact angles (blue triangles) of water on clean glass fibre as a function of time.

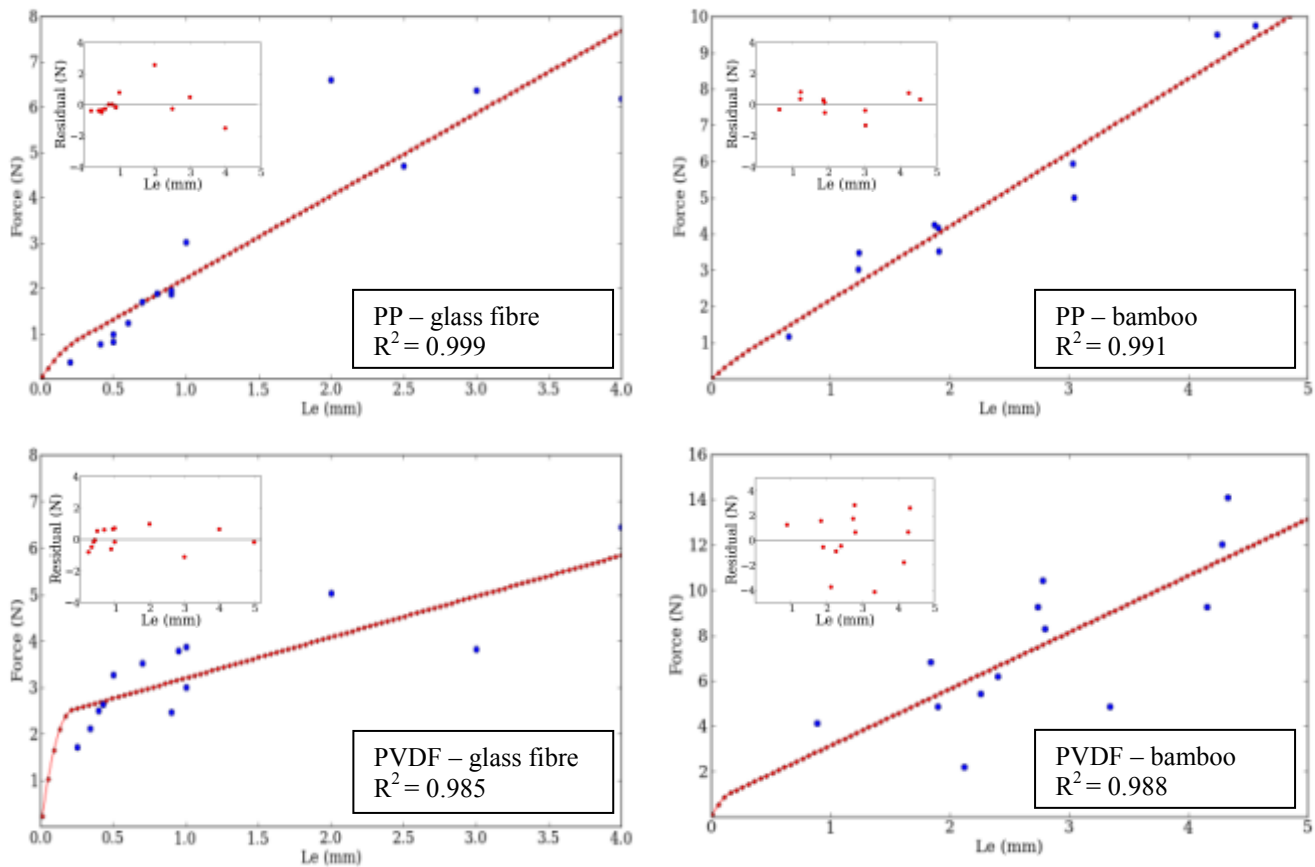


Figure 4. Experimental plot of the F_{max} versus the embedded length for glass (left) and bamboo (right) fibre systems, and their theoretical fits. The average bamboo fibre diameters were $244 \pm 26 \mu m$ and $241 \pm 36 \mu m$ for PP and PVDF respectively.

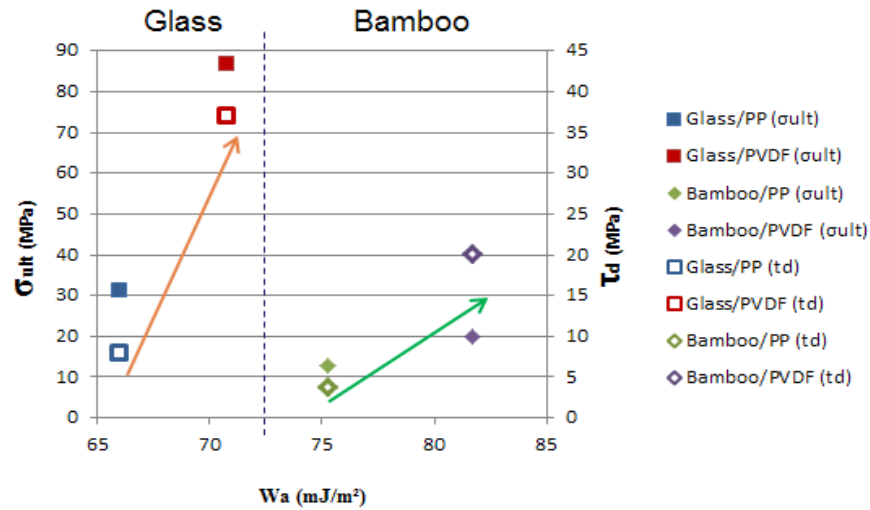


Figure 5. The correlation between interfacial parameters (τ_d and σ_{ult}) and W_a for glass and bamboo fibres, according to Table 3. The graphic shows that the higher W_a , the higher the interfacial parameters, if each system (glass and bamboo) is independently analysed. The arrows show the direct relationship.

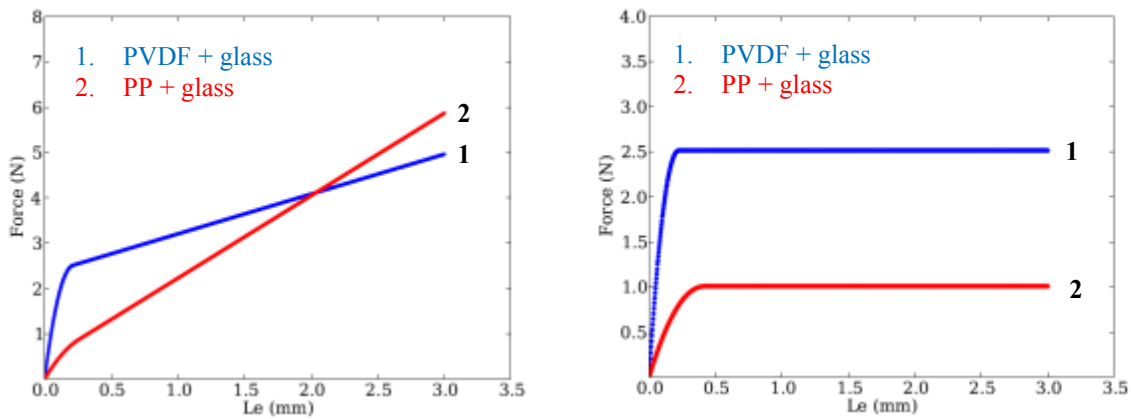


Figure 6. The maximum pull-out force plotted as function of the embedded length for glass systems. Left: the effect of friction is considered, right: friction is not considered. Curves are stress-based two-parameters best fits.

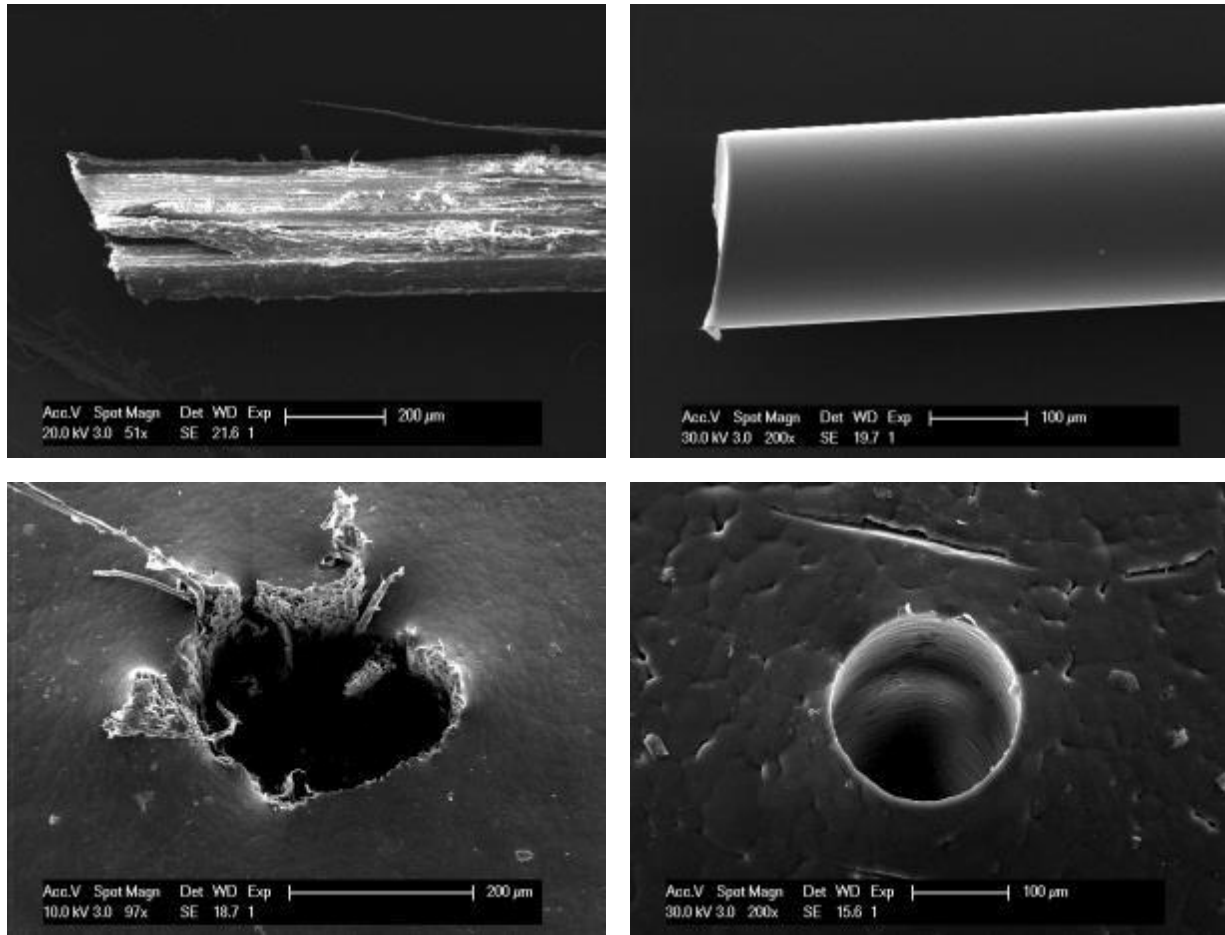


Figure 7. Pulled-out fibre (top) and pull-out hole (bottom) with PVDF as matrix. Left: bamboo, right: glass.

Table 1. Surface composition (molar fractions and molar ratios) determined using XPS for bamboo fibres and glass fibres, cleaned and stored in air or water.

Material	C (%)	O (%)	N (%)	Si (%)	O/C	O/Si	C/Si	Binding energy (eV)			
								284.8	286.3	287.6	289.0
								C1 (%)	C2 (%)	C3 (%)	C4 (%)
								(C-(C,H)) C-(Si-O)-C	(C-O,N)	(C=O, O-C-O)	(O-C=O)
Bamboo	74.3 ±1.5	22.9 ±0.3	1.8 ±0.7	0.6 ±0.4	0.3	38.2	123.8	58.0 ±3.1	28.8 ±2.3	7.6 ±1.3	5.6 ±0.4
Glass (air)	56.0 ±1.3	22.7 ±1.1	1.7 ±0.5	19.6 ±0.9	0.4	1.16	2.33	81.4 ±2.6	11.2 ±1.2	4.2 ±0.6	3.3 ±0.8
Glass (water)	31.1 ±1.1	41.2 ±1.8	0.8 ±0.2	26.9 ±0.6	1.3	1.53	0.88	75.6 ±1.8	16.7 ±1.7	4.1 ±0.3	3.6 ±0.5

Table 2. Contact angles (advancing, receding, and equilibrium) of test liquids on PP and PVDF films, and bamboo and glass fibres; and their surface energy components.

Material	WT			EG			DIO			SEC			
	Adv (°)	Rec (°)	Equ (°)	Adv (°)	Rec (°)	Equ (°)	Adv (°)	Rec (°)	Equ (°)	γ^{tot} (mJ/m ²)	γ^{LW} (mJ/m ²)	γ^+ (mJ/m ²)	γ^- (mJ/m ²)
PP	97.8 ±1.6	74.1 ±1.5	86.0 ±1.1	71.1 ±0.6	49.4 ±1.7	60.8 ±0.8	67.9 ±1.2	46.1 ±1.7	57.7 ±1.0	30.9 ±0.5	29.9 ±0.5	0.1 ±0.0	2.0 ±0.3
PVDF	85.5 ±0.9	68.9 ±1.2	77.3 ±0.7	54.1 ±1.2	32.1 ±1.6	44.2 ±0.9	63.6 ±0.4	46.5 ±1.8	55.5 ±0.8	34.6 ±0.5	31.2 ±0.5	0.9 ±0.1	3.3 ±0.2
Bamboo	--	--	47.2 ±2.1	--	--	33.4 ±1.8	--	--	32.5 ±2.3	45.3 ±1.2	43.2 ±1.0	0.1 ±0.0	14.5 ±1.2
Glass	36.5 ±1.4	23.1 ±0.5	30.5 ±1.1	41.3 ±2.0	20.2 ±2.6	32.2 ±2.1	61.8 ±1.7	54.2 ±1.5	58.1 ±1.6	40.5 ±2.1	29.7 ±0.2	1.1 ±0.2	27.3 ±0.1

Table 3. Interfacial and wetting parameters for bamboo and glass as substrates.

Material	τ_d (MPa)	τ_f (MPa)	σ_{ult} (MPa)	W_a (mJ/m ²)	S (mJ/m ²)	γ_{sl} (mJ/m ²)	ΔF (mJ/m ²)
PP+bamboo	3.8	2.7	12.85	75.27 ± 1.45	13.53 ± 1.45	0.91 ± 0.57	44.40 ± 1.17
PVDF+bamboo	13.8	3.3	20.11	81.71 ± 1.43	12.42 ± 1.43	-1.75 ± 0.51	47.06 ± 1.29
PP+glass	7.9	2.9	31.09	66.00 ± 0.99	4.26 ± 0.99	5.37 ± 0.35	35.13 ± 1.30
PVDF+ glass	37.0	1.4	86.76	70.76 ± 0.76	1.48 ± 0.76	4.38 ± 0.28	36.12 ± 0.36